

# Learning across scales - A multiscale method for Convolution Neural Networks

Eldad Haber\*, Lars Ruthotto†, Elliot Holtham‡

December 3, 2024

## Abstract

In this work we explore the connection between Convolution Neural Networks, partial differential equations, multigrid/multiscale methods and optimal control. We show that convolution neural networks can be represented as a discretization of nonlinear partial differential equations, and that the learning process can be interpreted as a control problem where we attempt to estimate the coefficients of the differential equations from data. This interpretation allows us to generate an efficient multilevel/multiscale process (sometimes referred to as image pyramid) and algorithms for the learning problem that can substantially reduce the cost of learning. Furthermore, this interpretation allows us to use the coefficients that are calculated on high resolution images for low resolution images directly.

## 1 Introduction

In this work we consider the problem of designing and optimizing convolutional neural networks (CNN). The topic has been a major field of research over the last years, after it has shown remarkable success in learning images of hand writing, natural images, videos and more (see for example [11, 10, 12] and references within). This

---

\*Department of Earth and Ocean Science, The University of British Columbia, Vancouver, BC, Canada

†Department of Mathematics and Computer Science, Emory University of British Columbia, Atlanta, GA, USA

‡Xtract technologies, Vancouver, BC, Canada

success has generated thousands of research papers and a few celebrated software packages.

However, the success of CNN's is not fully understood and in fact, tuning network structure and parameters is very hard in practice. The process requires many trial and error experiments to determine these parameters which can result in long training times and a lack of robustness. In many cases, small changes to the network can yield large changes in the learning outcome. This results in some sophisticated ideas that use Bayesian optimization techniques to infer the best architecture [7].

Current training methods depend on the architecture of the network, as well as the resolution of the image data. Changing resolution in either the training or prediction phase, is not easily accommodated with traditional CNN methods. In fact, the network is typically trained at some resolution, and the classification of new images requires the interpolation of the images to the resolution that the network was trained on. Such a process can be computationally expensive, particularly if the object under classification is a video or a 3D image (for example as commonly used in medical imaging and geosciences (see for example [8, 9])).

We focus our work on residual neural networks, where, a simple way to write the network is

$$\mathbf{y}_{k+1} = \mathbf{y}_k + F(\mathbf{y}_k, \boldsymbol{\theta}_k) \quad \mathbf{y}_0 = \mathbf{Lx} \quad (1.1)$$

Here,  $\mathbf{x}$  are the data and  $\mathbf{y} = [\mathbf{y}_1^\top, \dots, \mathbf{y}_n^\top]^\top$  are the hidden layers.  $\boldsymbol{\theta}_k = \{\mathbf{K}_k, \mathbf{b}_k\}$  are parameters (convolution kernels and biases) to be determined by the "learning" process. For simplicity we assume that  $\mathbf{y}_j$  is in  $R^m$  and the matrix  $\mathbf{L}$  maps the data vector  $\mathbf{x} \in R^s$  into the feature space  $\mathbf{y}$ . This matrix can be "learned" or fixed.

A common choice in CNN is to have the function  $F$  as a convolution with parameter  $\boldsymbol{\theta}$  that represent the convolution weights and bias, leading to the explicit expression

$$F(\mathbf{y}, \mathbf{K}, \mathbf{b}) = \sigma_\alpha(\mathbf{K}(\mathbf{s})\mathbf{y} + \mathbf{b}). \quad (1.2)$$

Here  $\mathbf{K}(\mathbf{s})$  is a convolution matrix, which is a circulant matrix that represents the convolution and depends on the stencil or convolution kernel,  $\mathbf{s}$ ,  $\mathbf{b}$  is a bias vector and  $\sigma_\alpha$  is an activation function. Note that for simplicity we have ignored the pooling layer, although it can be added in general (The necessity of pooling has been debated in [15]).

A classifier is obtained by propagating forward and using the last layer in some classification algorithm such as softmax, least squares, logistic regression or support vector machines. The classifier can be written as

$$\mathbf{z} = g(\mathbf{W}, \mathbf{y}_n). \quad (1.3)$$

Here  $g$  is a classification function and  $\mathbf{W}$  are classification weights. In supervised training, the **predicted** label  $\mathbf{z}$  is compared to a **known**, or observed label  $\mathbf{z}_{\text{obs}}$  and the different parameters,  $\mathbf{s}, \mathbf{b}$  and  $\mathbf{W}$  are tuned by an optimization algorithm such that  $\mathbf{z} \approx \mathbf{z}_{\text{obs}}$  for all known examples. In addition, some regularization may be added in order to avoid over fitting of the data. Typically, the problem is not solved to a high accuracy and low accuracy solutions are sufficient. A validation set is often used to determine the stopping criteria for the optimization algorithm.

In typical settings, the network is trained on image-data at some resolution, and therefore, the trained convolution stencil,  $\mathbf{s}$ , the classifier,  $\mathbf{W}$  and biasses  $\mathbf{b}$  are optimal to that particular resolution. The formulation does not easily extend between different resolutions. In particular, when changing the resolution of the image, it is not clear how to adopt the convolution kernel. Therefore, it is hard to use the process of multilevel continuation or image pyramid, where the network is trained at different resolutions. Such a process is known to be very efficient in other fields, both from a computational point of view, and from skipping local minima [13, 5, 1].

The goal of this paper is to enable multiscale computations in CNN's. At the heart of the process is the connection between the convolution, the discretization of differential operators and the prolongation and restriction of such operators on different meshes. Thus, in this paper we show that it is possible to interpret deep CNN's as a particular form of nonlinear time dependent partial differential equations. This understanding leads to a very common structure that is used in fields such as path planning, data assimilation and nonlinear Kalman filtering (see [2] and reference within). The embedding of CNN's in this framework allows for multiscale learning algorithms. In particular, it allows for the use of coarse scale training to initialize fine scale training. It also allows for the classification of low resolution images by networks that have been designed and trained on high resolution data *without* interpolation of the coarse scale image to finer scales.

The rest of this paper is structured as follows. In the next section, we show the connection between time dependent differential equations and CNN's. This connection allows us to introduce the optimization problem as a dynamic control problem. In Section 3 we briefly discuss the computation of derivatives and discuss our choice of optimization algorithm. In Section (4) we discuss the use of grid continuation for the efficient solution of the problem. Finally, in Section (6) we show a few examples and summarize the paper.

## 2 CNN's and partial differential equation

The deep convolution network has two components that we aim to give a different interpretation. The first is the spacial convolution and the second is the propagation from one layer to the next. In the next subsections we discuss the interpretation of convolution as differential operators and the depth of the layer as time propagation.

### 2.1 Convolution and differential operators

In this subsection we show that we can treat convolution as a discretization of a differential equation in space. This implicitly implies that the convolution kernel should be discretized differently, depending on the image resolution. Much of the discussion here can be found in classical partial differential equation and multigrid books such as [16].

To simplify the explanation, we start with a simple 1D example. Let us assume that  $\mathbf{y}$  is given on a mesh of size  $\Delta$  in some interval, and assume a simple single stencil or convolution kernel,  $\mathbf{s}$  of size  $3 \times 1$ .

It is simple to verify that the convolution between the vector  $\mathbf{s}$  and  $\mathbf{y}$  can also be written as

$$[\mathbf{s}_1 \mathbf{s}_2 \mathbf{s}_3] * \mathbf{y} = \frac{\alpha_1}{4} [1 \ 2 \ 1] * \mathbf{y} + \frac{\alpha_2}{2\Delta} [-1 \ 0 \ 1] * \mathbf{y} + \frac{\alpha_3}{\Delta^2} [-1 \ 2 \ -1] * \mathbf{y}$$

We see that

$$\begin{pmatrix} \mathbf{s}_1 \\ \mathbf{s}_2 \\ \mathbf{s}_3 \end{pmatrix} = \begin{pmatrix} \frac{1}{4} & -\frac{1}{2\Delta} & -\frac{1}{\Delta^2} \\ \frac{1}{2} & 0 & \frac{2}{\Delta^2} \\ \frac{1}{4} & \frac{1}{2\Delta} & -\frac{1}{\Delta^2} \end{pmatrix} \begin{pmatrix} \alpha_1 \\ \alpha_2 \\ \alpha_3 \end{pmatrix} \quad (2.4)$$

Since the matrix is invertible there is a one-to-one mapping between the sum of three convolutions to the original convolution.

All we did in the above is use different basis vectors to express the original convolution kernel. However, it is interesting to see that this basis can be interpreted in a different way. This is because, assuming that the vector  $\mathbf{y}$  is a discretization of a function  $y(x)$ , as the mesh size approaches 0 we have that

$$\begin{aligned} \lim_{\Delta \rightarrow 0} \frac{1}{4} (\mathbf{y}_{j-1} + 2\mathbf{y}_j + \mathbf{y}_{j+1}) &= y(x_j) \\ \lim_{\Delta \rightarrow 0} \frac{1}{2\Delta} (-\mathbf{y}_{j-1} + \mathbf{y}_{j+1}) &= \frac{dy}{dx}(x_j) \\ \lim_{\Delta \rightarrow 0} \frac{1}{\Delta^2} (\mathbf{y}_{j-1} - 2\mathbf{y}_j + \mathbf{y}_{j+1}) &= \frac{d^2y}{dx^2}(x_j). \end{aligned}$$

Therefore, a straight forward use of finite difference implies that for a piecewise smooth function  $y$  we have

$$\mathbf{s} * \mathbf{y} \approx \alpha_1 y + \alpha_2 \frac{dy}{dx} + \alpha_3 \frac{d^2 y}{dx^2},$$

where the vector  $\mathbf{y}$  is interpreted as a discretization (a grid function) of the function  $y(x)$ . Since images can be modeled as piecewise smooth functions (see for example [17, 4] and reference within) this representation of the kernel can be used across scales as typically done in multigrid and in image pyramid schemes.

Another interesting observation is that convolution windows that are bigger than 3 pixels, can be modeled either as a discretization of higher order differential operators, or as a number of 3-pixel convolutions. For example, a 5 window convolution can be modeled as a convolution with a window of 3 twice, and a 7 window convolution can be modeled as three times the convolution with a 3 pixel convolution.

It is easy to extend this process to 2 and 3D images with larger convolution stencils by using derivatives to other directions and higher order. In 2D we use the

stencils

$$\begin{aligned}
Id &\approx \frac{1}{16} \begin{pmatrix} 1 & 2 & 1 \\ 2 & 4 & 2 \\ 1 & 2 & 1 \end{pmatrix} & \frac{\partial}{\partial x} &\approx \frac{1}{6h} \begin{pmatrix} -1 & 0 & 1 \\ -2 & 0 & 2 \\ -1 & 0 & 1 \end{pmatrix} \\
\frac{\partial}{\partial y} &\approx \frac{1}{6h} \begin{pmatrix} -1 & -2 & -1 \\ 0 & 0 & 0 \\ 1 & 2 & 1 \end{pmatrix} \\
\frac{\partial^2}{\partial x^2} &\approx \frac{1}{4h^2} \begin{pmatrix} 1 & -2 & 1 \\ 2 & -4 & 2 \\ 1 & -2 & 1 \end{pmatrix} \\
\frac{\partial^2}{\partial y^2} &\approx \frac{1}{4h^2} \begin{pmatrix} 1 & 2 & 1 \\ -2 & -4 & -2 \\ 1 & 2 & 1 \end{pmatrix} \\
\frac{\partial^2}{\partial x \partial y} &\approx \frac{1}{h^2} \begin{pmatrix} -1 & 0 & 1 \\ 0 & 0 & 0 \\ 1 & 0 & -1 \end{pmatrix} \\
\frac{\partial^3}{\partial x^2 \partial y} &\approx \frac{1}{2h^3} \begin{pmatrix} -1 & 0 & 1 \\ 2 & 0 & -2 \\ -1 & 0 & 1 \end{pmatrix} \\
\frac{\partial^3}{\partial x \partial y^2} &\approx \frac{1}{2h^3} \begin{pmatrix} -1 & 2 & -1 \\ 0 & 0 & 0 \\ 1 & -2 & 1 \end{pmatrix} \\
\frac{\partial^4}{\partial x^2 \partial y^2} &\approx \frac{1}{2h^3} \begin{pmatrix} -1 & 2 & -1 \\ 2 & -4 & 2 \\ -1 & 2 & -1 \end{pmatrix}
\end{aligned}$$

as the basis for the convolution. It is straight forward to verify that these convolution kernels are linearly independent, and therefore represent a complete basis to span any  $3 \times 3$  convolution kernel.

Assume now that we are given some image data,  $\mathbf{y}_h$ , on a mesh with pixel size  $h$  and a convolution stencil,  $\mathbf{s}_h$  that operates on this image. Assume also that we would like to express the convolution on an image,  $\mathbf{y}_H$ , of different resolution, given by a coarser mesh of size  $H$ .

Let  $\mathbf{s}_H$  be the convolution kernel on mesh size  $H$ . The goal is to transfer the fine scale convolution stencil into the coarse one. This problem is well studied in the multigrid literature, with two possible solutions.

The first solution uses rediscritization to achieve this goal. That is, given  $\mathbf{s}_h$ , one computes the coefficients  $\boldsymbol{\alpha}$ . Since  $\boldsymbol{\alpha}$  is **mesh independent**, one can use the partial differential equation representation on every possible mesh. This approach is often referred to as rediscritization, and it is especially useful if the images are sufficient smooth.

A complementary view can be derived from an algebraic point of view, similar to algebraic multigrid methods [16]. To this end, we assume that the following connection holds between the fine mesh image,  $\mathbf{y}_h$ , and the coarse mesh image  $\mathbf{y}_H$ .

$$\mathbf{y}_H = \mathbf{R}\mathbf{y}_h \quad \text{and} \quad \tilde{\mathbf{y}}_h = \mathbf{P}\mathbf{y}_H \quad (2.5)$$

Here,  $\mathbf{P}$  is a prolongation matrix and  $\mathbf{R}$  is a restriction matrix.  $\tilde{\mathbf{y}}_h$  is an interpolated coarse scale image to the fine mesh and typically,

$$\mathbf{R}\mathbf{P} = \mathbf{I}.$$

The above interpretation is that the coarse scale image is obtained using some linear transformation from the fine scale image (e.g. averaging). Conversely, an approximate fine scale image can be obtained from the coarse scale image by interpolation. This interpretation can easily be extended to 3D for example for videos.

It is common to have  $\mathbf{P}$  as a linear interpolation, and  $\mathbf{R}$  as a full weight restriction [16]. For uniform nodal meshes, it is typical to have

$$\mathbf{P} = \gamma \mathbf{R}^\top,$$

with  $\gamma = 2^d$  a constant that depends on the dimensionality of the problem,  $d$ .

Let  $\mathbf{K}_h(\mathbf{s}_h)$  be the matrix that represents the convolution on the fine scale. This matrix operates on a vectorized image and is equivalent to convolving the vector  $\mathbf{y}_h$  with the stencil,  $\mathbf{s}_h$ . The matrix is circulant and sparse with a few non-zero diagonals. Our goal is to build a coarse scale convolution,  $\mathbf{K}_H$  that operates on a vector  $\mathbf{y}_H$  and is consistent with the operation of  $\mathbf{K}_h$  on a fine scale vector  $\mathbf{y}_h$ . Using the prolongation and restriction we obtain that

$$\mathbf{K}_H \mathbf{y}_H = \mathbf{R} \mathbf{K}_h \mathbf{P} \mathbf{y}_H. \quad (2.6a)$$

That is, given  $\mathbf{y}_H$  we first prolong it to the mesh  $h$ , then operate on it with the matrix  $\mathbf{K}_h$ , which yields a vector on mesh  $h$ . Finally, we restrict the result to the mesh  $H$ . This implies that the coarse scale convolution matrix can be expressed as

$$\mathbf{K}_H = \mathbf{R} \mathbf{K}_h \mathbf{P}. \quad (2.6b)$$

This definition of the operator can be built directly using any interpolation/restriction operators. Furthermore, assuming that the convolution stencil,  $\mathbf{s}_H$  is constant on the coarse mesh (that is, it is not changing on the mesh as commonly assumed in CNN), it is straight forward to evaluate it without generating the matrix  $\mathbf{K}_H$ , as commonly done in algebraic multigrid.

To demonstrate the concept of how the convolution changes with resolution, we use the following simple example demonstrated in Figure 1. We select an image from the MNIST data set (bottom left) and convolve it with the weights

$$\mathbf{s}_h = \begin{pmatrix} -0.89 & -2.03 & 4.30 \\ -2.07 & 0.00 & -2.07 \\ 4.39 & -2.03 & 1.28 \end{pmatrix}$$

obtaining the image in the bottom right panel of Figure 1.

Restricting the weights using the algebraic multigrid approach, we obtain that on a coarse mesh the weights are

$$\mathbf{s}_H = \begin{pmatrix} -0.48 & -0.17 & 0.82 \\ -0.15 & -0.80 & 0.37 \\ 0.84 & 0.40 & 0.07 \end{pmatrix}.$$

These weights are used on the coarse scale image (top left panel of Figure 1) to construct the filtered image on the top right panel of Figure 1. Looking at the weights obtained on the coarse mesh, it is evident that they are significantly different from the fine scale weights. It is also evident from the fine and coarse images, that adjusting the weights on the coarse mesh is necessary if we are to keep a faithful transformation between the images.

The interpretation of convolutions as differential operators and its algebraic equivalent, allows us to work with different resolutions. This has two important consequences. First, assume that we have trained our network on some fine scale images and that we are given a coarse scale image. Rather than interpolating the image to a fine mesh (which can be memory intensive and computationally expensive), we transform the **stencils** to a coarse mesh and use the coarse mesh stencils to classify the coarse scale image. Such a process can be particularly efficient when considering the classification of videos on mobile devices where expanding the video to high resolution can be computationally prohibitive. A second consequence is that we are able to train the network on a coarse mesh and then interpolate the result to a fine mesh. As we see next, this allows us to use a process of image pyramid or multiresolution for the solution of the optimization problem that is at the heart of the training process.

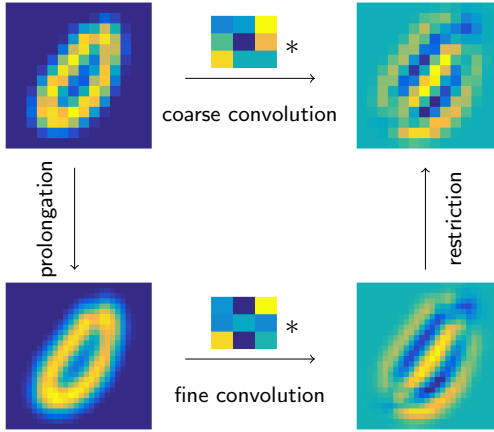


Figure 1: Illustration of a fine mesh vs. coarse mesh convolution.

## 2.2 Propagation and time dependent differential equations

Interpreting the convolution as a differential operator is a first step in presenting CNN's as a continuous structure. Next, we interpret the depth of the network in a continuous framework.

We start by rewriting the CNN model as a residual CNN as suggested in [6].

$$\mathbf{y}_{j+1} - \mathbf{y}_j = \sigma_\alpha(\mathbf{K}_j \mathbf{y}_j + \mathbf{b}_j). \quad (2.7)$$

The difference on the left hand side of the above equation, is nothing but an approximation to the derivative  $\partial_t \mathbf{y}$  with step size 1. This approximation is valid if  $\mathbf{y}$  changes sufficiently slowly. Nonetheless, if  $\mathbf{y}$  changes quickly, then the discrete system may be chaotic. Having a chaotic system as a forward problem implies that one can expect difficulties when considering the inverse problem. Therefore, our first goal is to stabilize the forward propagation process. To this end, we propose a *continuous* time dependent processes that generalizes Equation (2.7).

$$\dot{\mathbf{y}}(t) = \sigma_\alpha(\mathbf{K}(t)\mathbf{y}(t) + b(t)) \quad (2.8a)$$

$$\mathbf{y}(0) = \mathbf{y}_0. \quad (2.8b)$$

General stability of ordinary differential equations (ODE's) apply for this process and in particular, it is easy to verify that the system of ODE's is stable as long as the real part of the eigenvalues of  $\mathbf{K}$  are not positive. A second well known problem is vanishing derivatives. This implies that the eigenvalues of  $\mathbf{K}$  have a strong negative

real part. Note that if the eigenvalues of  $\mathbf{K}$  are imaginary, then no decay of the signal occurs, and no vanishing gradients are expected. This can aid in choosing and initializing the network parameters.

Many discretization techniques can retain the network stability (assuming that the continuous network is well posed). Perhaps the simplest discretization of this ODE is the forward Euler method, leading to the discrete dynamical system

$$\mathbf{y}_{j+1} = \mathbf{y}_j + \delta t \sigma_\alpha (\mathbf{K}_j \mathbf{y}_j + \mathbf{b}_j) \quad (2.9)$$

which is stable as long as  $\delta t$  is sufficiently small and  $\mathbf{K}$  does not contain positive eigenvalues. This generalizes residual networks to a continuous process that is amendable to numerical modeling.

### 2.3 Space-time formulation

We now combine the space-time interpretation and the classification to give the deep CNN a continuous interpretation.

We assume to have continuous (in space) data and a mapping from this data to the 0<sup>th</sup> feature space  $y_0$ . The feed forward problem can now be written as

$$\begin{aligned} \frac{\partial y}{\partial t} &= \sigma_\alpha \left( \sum_j \theta_j(t) D_j y(t, x) + b(t) \right) \\ y(0, x) &= y_0(x), \quad y \in \Omega \times [0, 1] \end{aligned} \quad (2.10)$$

Here,  $D_j$  are differential operators that correspond to the order of the differential equation to be solved and the dimension of the problem. For problems in 2D with  $3 \times 3$  convolution kernels  $D_j$  are given operators up to second derivatives in each direction.

The learning problem can now be formulated as a path control problem. Assuming we have different initial conditions  $\{y_0^{(1)}, \dots, y_0^{(s)}\}$ , our goal is to generate a dynamical system that separates these conditions into classes. Let  $g(W, y^\ell(1))$  be a classifier. For example, a simple classifier can be represented by the integral

$$\mathbf{z}^{(\ell)} = \int_{\Omega} W \cdot y^{(\ell)}(t = 1) d\vec{x} \quad (2.11)$$

Let  $\mathbf{z}_{\text{obs}}^{(\ell)}$  be the label of the  $\ell$  data.

The simplest learning process using  $L_2$  misfit function can now be formulated as a control problem of the form

$$\begin{aligned} \min_{\theta_j, b, W} \quad & \frac{1}{2} \sum_{\ell=1}^s \|\mathbf{z}^{(\ell)} - \mathbf{z}_{\text{obs}}^{(\ell)}\|^2 \\ \text{s.t.} \quad & \frac{\partial y}{\partial t} = \sigma_\alpha \left( \sum_j \theta_j(t) D_j y + b(t) \right) \\ & y(0) = y_0^{(\ell)} \quad \ell = 1, \dots, s. \end{aligned} \quad (2.12a)$$

It is easy to change the learning criteria from  $L_2$  to others such as soft-max but for simplicity we discuss the  $L_2$  criteria.

Although we never work in the continuum, the continuous model can aid in a number of ways. First, it gives a framework to solve the problem that is shared with many other fields such as optimal control, data assimilation, weather forecasting and path planning. It allows us to borrow some of the algorithms used in these fields in order to have efficient computations. Most importantly, the continuous mathematical structure allows us to use a continuation model in time (which corresponds to adding hidden layers) and in space (multi-resolution). This can help to significantly reduce the computational cost as commonly done in other space-time control problems.

### 3 Calculation of sensitivities and optimization

Equation (2.9) can now be used to generate an efficient learning process. To do this, we briefly discuss the computation of the sensitivity matrix and our choice of optimization algorithm.

Let  $\mathbf{Y}_j = [\mathbf{y}_j^1, \dots, \mathbf{y}_j^s]$ , that is,  $\mathbf{Y}_j$  is a matrix that contains the states at time step  $j$  for all training examples. Using the explicit formula (1.1), it is straight forward to verify that the derivatives of  $\mathbf{Y}_{j+1}$  with respect to  $\mathbf{K}$  and to  $\mathbf{Y}_j$  are

$$\begin{aligned} \frac{\partial \text{vec}(\mathbf{Y}_{j+1})}{\partial \text{vec}(\mathbf{K}_j)} &= \mathbf{I} + \delta t \text{diag}(\sigma'_\alpha(\mathbf{K}_j \mathbf{Y}_j + b_j)) (\mathbf{Y}_j^{top} \otimes \mathbf{I}) \\ \frac{\partial \text{vec}(\mathbf{Y}_{j+1})}{\partial \text{vec}(\mathbf{Y}_j)} &= \mathbf{I} + \delta t \text{diag}(\sigma'_\alpha(\mathbf{K}_j \mathbf{Y}_j + b_j)) (\mathbf{I} \otimes \mathbf{K}_j) \end{aligned} \quad (3.13)$$

where the operation  $\text{vec}(\mathbf{Y})$  rearrange the matrix  $\mathbf{Y}$  into a vector. As usual, derivatives can be obtained in a forward or a backward manor using the chain rule.

It is important that the matrices in Equation (3.13) need not be formed or stored. A matrix-vector product can be efficiently computed by noting that, for an arbitrary vector  $\mathbf{V}$ , we have that

$$\begin{aligned} \frac{\partial \text{vec}(\mathbf{Y}_{j+1})}{\partial \text{vec}(\mathbf{K}_j)} \text{vec}(\mathbf{V}) = \\ \text{vec}(\mathbf{V} + \delta t (\sigma'_\alpha (\mathbf{K}_j \mathbf{Y}_j + b_j)) \odot (\mathbf{V} \mathbf{Y}_j)). \end{aligned}$$

This implies that we can compute matrix vector products using dense-dense operations on many samples. Similar expressions can be obtained for the computation of matrix vector products of the transpose of the matrices with a vector.

Let us now consider the solution of the optimization problem of minimizing a loss function with respect to the classification weights  $\mathbf{W}$ , the convolution stencils  $\mathbf{s}$ , and the biases.

While it is possible (and common) to use stochastic first order methods, we use stochastic second order methods. Advantages of second order methods have been recently explored in [3] and in [14]. We use the Gauss-Newton-CG method on large batches of data.

At each iteration of the method we compute the gradient and approximately solve the Gauss-Newton system using conjugate gradient.

It is important to note that no Hessian or Jacobian is computed explicitly and only matrix-vector products are needed for the computation. Also, Newton-type methods do not require a “learning rate” or momentum and they naturally scale, which makes the optimization algorithm much more robust. We refer to [3] and in [14] for an elaborate discussion.

## 4 Multiscale optimization and mesh continuation

Understanding how to move between different scales allows us to construct efficient algorithms that use inexpensive coarse mesh representations of the problem in order to initialize the problem on finer scales. This is similar to the classical image pyramid process [5] and multilevel methods that are used in applications that range from full waveform inversion to shape from shading [18]. The idea is to solve the optimization problem on a coarse mesh first in order to initialize fine grid parameters. The algorithm is summarized in Algorithm 1.

Solving each optimization problem on coarser meshes is cheaper than solving the problem on finer meshes. In fact, when an image is coarsened by a factor of 2, each

---

**Algorithm 1**

---

- 1: Restrict the images  $n$  times
- 2: Initialize the convolution kernels and classifiers
- 3: **for**  $k = n : -1 : 1$  **do**
- 4:     Solve the optimization problem (2.12) on mesh  $k$  from its initial point
- 5:     Prolong the convolution kernel to level  $k - 1$
- 6:     Update the classifier weights
- 7: **end for**

---

convolution step is 4 times cheaper in 2D and 8 times cheaper in 3D. In some cases, such a process leads to linear complexity of the problem [16].

In order to apply such algorithms in our context, we need to address the transformation of the coarse scale operator to a fine scale one. This process is different than classical multigrid where the operator on a fine mesh is given, and a coarse scale representation is desired. As previously discussed, we use the classical multigrid result to transform a fine mesh operator to a coarse one

$$\mathbf{K}_H = \mathbf{R}\mathbf{K}_h\mathbf{P}. \quad (4.14)$$

In the classical multigrid implementation, one has a hold on the *fine scale* operator  $\mathbf{K}_h$ , and the goal is to compute the coarse scale operator  $\mathbf{K}_H$ . In our application, throughout the mesh continuation method, we are given the *coarse mesh* operator and we are to compute the fine mesh operator. In principle, there is no unique fine scale operator given a coarse scale one; however, assuming that the fine scale operator is a convolution with fixed stencil (as in the case of CNN), there is a unique solution. This is a classical result in Fourier analysis on multigrid methods [16]. Since (4.14) represents a linear connection between  $\mathbf{K}_h$  and  $\mathbf{K}_H$ , we extract  $n_K^2$  equations (where  $n_K$  is the size of each convolution kernel) that connect the fine scale convolutions to the coarse scale ones. For a convolution kernel of size  $3^2$  and linear prolongation/restriction, this is a simple  $9 \times 9$  linear system that can be easily solved to obtain the fine scale convolution. A classical multigrid result is that this linear system is well-posed. Assuming that the coarse mesh is a  $n_K \times n_K$  stencil and that the interpolation is linear, the fine mesh stencil is also a  $n_K \times n_K$  stencil which is uniquely determined from the coarse mesh stencil.

## 5 Examples

In this section we demonstrate the potential of our method using the MNIST dataset that consists of 60,000 labeled images each with  $28 \times 28$  pixels.

Since the images are rather coarse, we use only two levels. To obtain coarse scale images the fine scale images are convolved with a Gaussian, and restricted to a coarse mesh using the operator introduced above. This yields a coarse mesh data consisting of  $14 \times 14$  images. We randomly divide the datasets into a training set consisting of 40,000 images, and a validation set consisting of 20,000 images. In all experiments, we choose a CNN with 2 layers and a least-squares classifier. We first choose random kernels, and then solve for the classifier weights. This is a simple convex problem that requires little computations and can be solved on the entire data set. We then compare the improvements in classification after the computation of the kernels.

For comparison of the different methods, we train the CNN on the fine level. The pure fine level training error reduces the objective function by about 62.4% from about 0.218 to 0.082. The classification accuracy on the testing set is increased from 82.9% to 96.7%.

### 5.1 Multilevel CNN Training

We demonstrate the computational benefit of coarse mesh training compared with only training the fine mesh CNN. The first step is coarse mesh training. To this end, we restrict the fine mesh feature maps to the coarse mesh using the operator  $\mathbf{R}$  introduced above. We then performed 10 iterations of a block coordinate descent methods that first approximately solves the convex problem for the classification weights, and secondly approximately solves the nonlinear optimization problem for the kernels using two-iterations of a randomized Gauss-Newton with a batch size of 10,000 images. Doing so reduces the coarse mesh objective function by approximately 62.8% from about 0.212 to 0.081. The classification accuracy measured on the validation set increases from 82% to 96.4%.

In a subsequent step, we use the coarse mesh result as a starting point for the fine mesh problem. To this end, we compute the equivalent fine mesh operator for the coarse mesh stencils using the algebraic techniques introduced above. We then solved for the classification weights and finally used the Gauss-Newton method.

Using the prolonged stencil gives an initial (essentially free) reduction of the objective function of 35.5% from around 0.218 to 0.147 (correspondingly, the classification accuracy on the validation set improves from 87% to 92% ). Due to the good starting guess, the fine mesh problem converges relatively quickly and yields

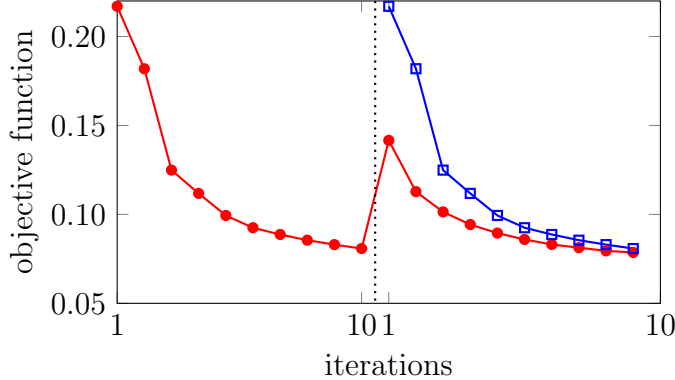


Figure 2: Multilevel convergence. The objective function value is shown at each outer iteration for fine scale training (blue squares) and multilevel learning (red dots). The dashed vertical line shows the transition from the coarse to fine mesh. The added benefit of multilevel training is evident by comparing the objective function values at the first iteration of the fine mesh for both schemes.

a trained CNN with an accuracy of 96.7%. The convergence of the method can be seen in Fig. 2.

## 5.2 Coarse Mesh Classification using Fine Mesh CNN

We demonstrate that using the continuous formulation we are able to classify coarse mesh images using a fine mesh CNN *without* using fine mesh convolution and any coarse level training. This is important for efficient classification on mobile devices etc.

First, we restrict the classification weights and kernels obtained on the fine mesh using the restriction operator explained above. Here, we use the results from the single-level fine mesh learning (thus, the coarse mesh data was not used). On the coarse mesh images, we apply the CNN for 20,000 randomly chosen images from the data set. This way we obtain a classification accuracy of 84.1% *without* training on the coarse data and *without* using any fine mesh convolutions. As to be expected due to the coarsening of the data the classification is less accurate than using a CNN trained on that resolution.

In our experience, the consistent prolongation of the kernel is of key importance. In the example at hand, using the restricted classification weights with the fine mesh kernels gives an accuracy of 81.8%, which is inferior. Note that prolongating the

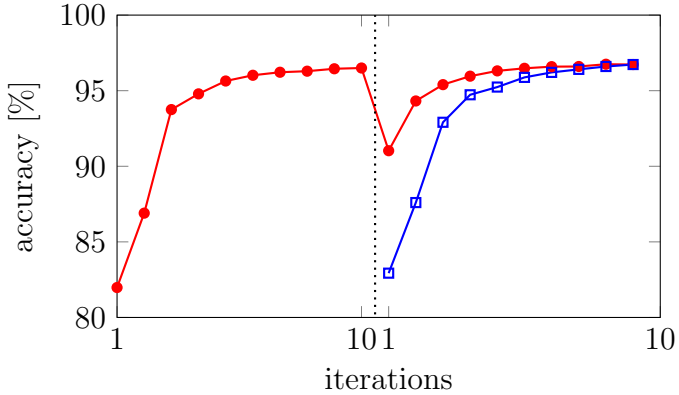


Figure 3: Classification accuracy for fine-level and multi-level learning. The accuracy is shown at each outer iteration during the fine scale training (blue squares) and multilevel learning (red dots). The dashed vertical line shows the transition from the coarse to fine mesh. The added benefit of the multilevel training is evident by comparing the accuracy at the first iteration of the fine mesh for both schemes.

kernels does not involve any significant computation (runtime with our prototype implementation was 0.03 seconds).

## 6 Conclusions

In this work, we have explored a new formulation that allows learning across scales. The foundation of our approach is the embedding of deep CNN’s in nonlinear partial differential equations. This mathematical structure allows the use of multilevel approaches that are commonly used for the numerical solution of partial differential equations. This approach enables us to define coarse and fine mesh convolutions that are consistent with coarse and fine scale images.

We then use our approach in two ways. First, we demonstrate that it is possible to use coarse representation of the images to learn the convolution kernels and prolong them into the fine representation of the same images. The prolongation uses either the differential form of the convolution kernel, or the interpolation and restriction matrices that are used to interpolate the images. A second consequence of our work is the ability to learn the kernels on some fine resolution and then restrict them to any resolution, allowing the use of trained results on fine images to be used on coarse ones. This can have a significant advantages for problems where memory is an issue

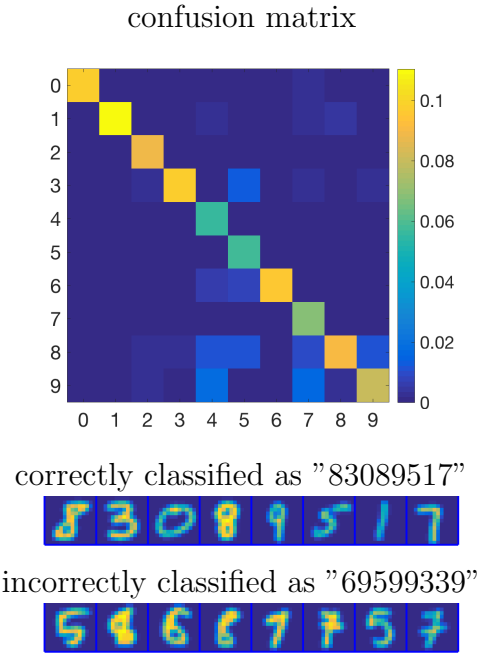


Figure 4: Classifying coarse mesh images using fine mesh CNN. Top shows confusion matrix for restriction of fine mesh CNN. The restriction allows to classify coarse data with an accuracy of around 84.1% *without* coarse mesh training or fine mesh convolution. Clearly the restriction leads to a loss of information and problems in the classification of similar digits as can be seen in the bottom plot.

and interpolation of images or videos is not practical.

Casting CNN's as an optimization problem with differential equations can give a different representation of the kernels, and to explicitly regularize the problem and obtain further insight into the field.

## References

- [1] M. Warner and A. Ratcliffe, T. Nangoo, J. Morgan, A. Umpleby, N. Shah, V. Vinje, I. Štekl, L. Guasch, C. Win, G. Conroy, and A. Bertrand. Anisotropic 3d full-waveform inversion. *GEOPHYSICS*, 78(20):59–80, 2013.
- [2] L. T. Biegler, O. Ghattas, M. Heinkenschloss, D. Keyes, and B. van Bloemen Waanders (Editors). *Real-Time PDE-Constrained Optimization*. SIAM,

Philadelphia, 2009.

- [3] L. Bottou, F. E. Curtis, and J. Nocedal. Optimization Methods for Large-Scale Machine Learning. *ArXiv e-prints*, June 2016.
- [4] T. Chan and J. Shen. Mathematical models for image inpainting. *SIAM J. Appl. Math.*, 23, 2001.
- [5] E. Haber and J. Modersitzki. Multilevel methods for image registration. *SIAM J. on Scientific Computing*, 27:1594–1607, 2004.
- [6] Kaiming He, Xiangyu Zhang, Shaoqing Ren, and Jian Sun. Deep residual learning for image recognition. *CoRR*, abs/1512.03385, 2015.
- [7] José Miguel Hernández-Lobato, Michael A. Gelbart, Ryan P. Adams, Matthew W. Hoffman, and Zoubin Ghahramani. A general framework for constrained bayesian optimization using information-based search. volume 17, pages 1–53, 2016.
- [8] J. Jiang, P. Trundle, and J. Ren. Medical image analysis with artificial neural networks. *Computerized Medical Imaging and Graphics*, 34:617631, 2010.
- [9] Andrej Karpathy, George Toderici, Sanketh Shetty, Thomas Leung, Rahul Sukthankar, and Li Fei-Fei. Large-scale video classification with convolutional neural networks. In *CVPR*, 2014.
- [10] A. Krizhevsky, I. Sutskever, and G. Hinton. Imagenet classification with deep convolutional neural networks. *Advances in neural information processing systems*, 61:10971105, 2012.
- [11] Y. LeCun and Y. Bengio. Convolutional networks for images, speech, and time series. *The handbook of brain theory and neural networks*, 3361:255258, 1995.
- [12] Y. LeCun, K. Kavukcuoglu, and C. Farabet. Convolutional networks and applications in vision. *IEEE International Symposium on Circuits and Systems: Nano-Bio Circuit Fabrics and Systems*, page 253256, 2010.
- [13] J. Modersitzki. *Numerical Methods for Image Registration*. Oxford, 2004.
- [14] F. Roosta-Khorasani and M. W. Mahoney. Sub-Sampled Newton Methods II: Local Convergence Rates. *ArXiv e-prints*, January 2016.

- [15] Jost Tobias Springenberg, Alexey Dosovitskiy, Thomas Brox, and Martin A. Riedmiller. Striving for simplicity: The all convolutional net. *CoRR*, abs/1412.6806, 2014.
- [16] U. Trottenberg, C. Oosterlee, and A. Schuller. *Multigrid*. Academic Press, 2001.
- [17] L. Vese and T. Chan. A multiphase level-set framework for image segmentation using the mumford and shah model. *Int. J. of Comp. Vision*, 50(3):271–279, 2002.
- [18] Ruo Zhang, Ping-Sing Tsai, James Cryer, and Mubarak Shah. Shape from shading: A survey. *IEEE Transactions on Pattern Analysis and Machine Intelligence*, 21-8:690–706, 1999.